On Hierarchical Network Coding Versus Opportunistic User Selection for Two-Way Relay Channels with Asymmetric Data Rates

Xuehua Zhang, Ali Ghrayeb, and Mazen Hasna

***Abstract*—We address in this paper the challenge of coping with asymmetric data rates in two-way relay channels. We consider a relay network comprising two sources and one relay. The sources communicate at different rates through the relay. That is, we assume that one source uses M_1-QAM (quadrature amplitude modulation) and the other uses M_1/M_2-QAM hierarchical modulation where $M_1 \neq M_2$. For the underlying network, we consider two decode-and-forward (DF) relaying schemes. One scheme combines hierarchical zero padding and network coding (HZPNC) at the relay. The novelty of this scheme lies in the way the two signals (that have different lengths) are network-coded at the relay. The other scheme is referred to as opportunistic user selection (OUS) where the user with a better end-to-end channel quality is given priority for transmission. We analyze both schemes where we derive closed-form expressions for the end-to-end (E2E) bit error rate (BER). Since the two schemes offer a trade-off between performance and throughput, we analyze and compare both schemes in terms of channel access probability and average throughput. We show that HZPNC offers better throughput and fairness for both users, whereas OUS offers better performance. We also compare the performance of HZPNC with existing schemes including the original zero padding, nesting constellation modulation and superposition modulation. We show through examples the superiority of the proposed HZPNC scheme in terms of performance and/or reduced complexity.**

***Index Terms*—Asymmetric data rates, cooperative diversity, decode-and-forward relaying, hierarchical modulation, two-way relay channel.**

I. Introduction

COOPERATIVE communications has proven to be an effective way to combat wireless fading by allowing the mobile nodes to share their antennas to achieve spatial diversity [1]-[3]. However, for practical reasons, cooperative nodes should operate in a half-duplex mode [3], implying a loss in spectral efficiency. In order to mitigate the spectral efficiency loss and improve the throughput of cooperative communication networks, some efforts have been made to incorporate network coding (NC) into cooperative communication. The concept of NC was first proposed by Ahlswede, *et. al*. in [4] as a routing method in lossless wireline networks. The key idea of NC is that an intermediate node, normally referred to as a relay node, linearly combines the received data from different sources instead of sending them individually, resulting in an improved bandwidth efficiency. Applying NC comes naturally due to the broadcast nature of wireless communications where multiple destinations can receive the same signal at the same time.

A variety of NC schemes have been proposed and studied in the literature for different network settings [5]–[21]. However, much attention in this field has been given to half-duplex two-way relaying as it is a basic building block of most wireless networks [8]-[21]. Various NC protocols have been proposed for this two-way relaying channel. Such protocols can be classified into two types: two time-slot NC schemes (i.e., analog network coding [8]-[10] and physical-layer network coding [11]-[14]) and three time-slot NC schemes [15]. The three time-slot NC scheme has been extensively studied in [16]-[19]. This NC scheme combined with threshold-based relaying to control error propagation with maximum ratio combining (MRC) has been studied in [17], and with maximum likelihood (ML) detection in [18]. In [16], the authors address the problem of relay assignment for cooperative networks comprising multiple bidirectional transmitting pairs. The problem of relay selection is addressed in [19] and references therein. In most of the work mentioned above that deals with bidirectional transmission, it is normally assumed that the two transmitting nodes (or users) have the same rate. In many practical scenarios, however (such as having different quality of service (QoS) requirements, different available traffic and so on), the two users may not have the same transmission rate. In light of this, the immediate question that comes to mind is how the relay nodes can cope with this data rate asymmetry without sacrificing the bandwidth efficiency. This is one of the problems that we address in this paper.

In this work, we consider a cooperative network comprising two users and an intermediate relay node. The users are assumed to have different data rates. Without loss of generality, and for ease of presentation, we assume that one user uses 4-QAM (quadrature amplitude modulation) and the other uses 16-QAM (we also consider 64-QAM later on.). The relay receives and decodes the bits received from both users in the first two time-slots.[1] In the third time-slot, the relay applies exclusive-or (XOR) to both bit streams and broadcasts the

Manuscript received October 19, 2012; revised February 13, 2013. The editor coordinating the review of this paper and approving it for publication was C. Ling.

This paper was made possible by NPRP grant 08-055-2-011 from the Qatar National Research Fund (a member of the Qatar Foundation). The statements made herein are solely the responsibility of the authors.

X. Zhang is with the ECE Department, Concordia University, Montreal, Canada (e-mail: xuehua08@gmail.com).

A. Ghrayeb is with the ECE Department, Texas A&M University at Qatar, Doha, Qatar, on leave from Concordia University, Montreal, Canada (e-mail: ghrayebali@gmail.com).

M. Hasna is with the EE Department, Qatar University, Doha, Qatar (e-mail: hasna@qu.edu.qa).

Digital Object Identifier 10.1109/TCOMM.2013.052013.120790

[1] A time-slot in this context implies the time required to transmit an entire frame.

0090-6778/13$31.00 © 2013 IEEE

resulting bit stream to both nodes. Since the data sequence lengths received at the relay are different, we can not apply XOR network coding directly. In [20], the author tried to solve the rate mismatch by reinterpreting network coding as a mapping of modulation constellation. However, this joint modulation/NC approach requires considerable changes to the de(modulator) design and increases the detection and demodulation complexity. In contrast, one simple way, without increasing the complexity of demodulation, is to append zeros to the end of the shorter bit sequence to make the two bit sequences have the same length. This zero padding process suggests that both users need to operate at 16-QAM which will deteriorate the performance of the system.

To remedy the rate mismatch challenge without much performance degradation, we propose to use $4/16$-QAM hierarchical modulation [22]-[24] at both the source and relay. The $4/16$-QAM hierarchical modulation consists of two different transmission priorities for the data stream, high priority (HP) bits and low priority (LP) bits. Specifically, the bit stream corresponding to the user using 16-QAM is divided into two substreams, high and low priority. At the relay, the HP substream is XORed with the 4-QAM stream coming from the second user, and the LP substream is unchanged. Therefore, the proposed NC scheme can be viewed as modified zero padding. The difference between the original zero padding and the proposed one is that the zeros are added at specific positions in the latter case. At the destination of the user employing 4-QAM, it only needs to decode the high priority bits which corresponds to a fictitious 4-QAM constellation instead of 16-QAM constellation. Compared to the original zero padding scheme, the complexity of the proposed scheme remains unchanged while the performance is improved. In addition, employing hierarchical modulation gives more freedom to adjust the end-to-end (E2E) performance of the two users by adjusting the relative distances between the constellation points. We hereafter refer to the proposed scheme as hierarchical zero padding/network coding (HZPNC).

We point out that we are not the first to relate hierarchical modulation to network coding. In fact, the authors in [21] propose to use $4/16$-QAM hierarchical modulation at the source to cope with the performance degradation caused by asymmetric relay channels. Comparing our work with [21], there are three main differences. Firstly, the problem we address here is how to cope with the data rate mismatch at the relay, while in [21], the authors address the problem of how to avoid performance degradation caused by asymmetric relay channels. Secondly, the scheme proposed in [21] relies on the direct path to alleviate the problem of asymmetric relay channels, rendering that scheme inapplicable in the absence of the direct path. There is no such constraint for our scheme. Finally, since the direct path can not be utilized for MRC detection at the destination for the scheme proposed in [21], one user will only have diversity order one although the direct path is available. For our scheme, however, both users are expected to achieve diversity order two in case the direct path is available.

On another relevant aspect, two-way relay channels have been studied in the context of multiuser systems. Specifically, in the presence of multiple users, only the user with the best E2E instantaneous SNR transmits and the rest remain silent until their channels improve. In [25] and [26], the authors studied the performance of this scheme for AF relaying. It is shown that higher reliability is achieved. In this paper, we extend this scheme to the DF relaying case, and we refer to it as opportunistic user selection (OUS). The reason for considering OUS here is that it provides another solution to the data rate mismatch problem, which renders itself a competitor for the proposed HZPNC scheme. Obviously there is a sharp contrast between the two schemes. For instance, OUS is expected to achieve better performance compared to the HZPNC scheme due to the multiuser diversity. However, the performance improvement comes at the expense of using more time slots as compared to HZPNC, as well as failing to achieve fairness among users. We study the performance of both schemes over independent Rayleigh fading channels. We derive closed-form expressions for the exact E2E bit error rate (BER) performance. We also study the access probability of OUS since it lacks fairness among users. A performance comparison between HZPNC and existing schemes such as zero padding, nesting constellation modulation and superposition modulation [6] is given to demonstrate the superiority of the HZPNC scheme. We present several examples through which we validate the theoretical results.

In light of the above discussion, the contributions of the paper may be summarized as follows:

1) We propose the HZPNC scheme to cope with the data rate mismatch problem at the relay. This involves employing hierarchical modulation by the user with the higher data rate and at the relay, while padding zeros at specific positions of the shorter bit sequence at the relay. The proposed scheme outperforms other existing schemes such as the original zero padding scheme, nesting constellation modulation and superposition modulation in terms of the BER performance and/or complexity.
2) We analyze the OUS scheme with DF relaying, assuming asymmetric data rates, and compare its performance to that of the HZPNC scheme in terms of BER performance, access probability and throughput.
3) We derive the probability density function (PDF) of the SNR for each hop with asymmetric channels. We derive closed-form expressions for the E2E BER performance for HZPNC, OUS, and the original zero padding. We also derive expressions for the access probability and throughput for the HZPNC and OUS schemes.

The remainder of the paper is organized as follows. The system model is presented in Section II. In Section III, the proposed HZPNC and OUS schemes are presented. We analyze the E2E BER performance of the two proposed schemes in Section IV. We compare the HZPNC and OUS schemes in terms of access probability and throughput in Section V. We present several numerical examples in Section VI, and Section VII concludes the paper.

II. System Model

We consider a bidirectional cooperative network with two users denoted by S_1 and S_2, and one relay denoted by R,

where the users communicate with each other via the relay node over orthogonal subchannels. For simplicity, we assume that there is no direct path between the two users. Both users and the relay are equipped with a single antenna and operate in a half-duplex mode. The two users have different data rates. In particular, we assume that one user uses 4-QAM and the other uses 16-QAM. (We also give results for the case when the second user uses 64-QAM.)

The network subchannels are assumed to experience independent slow and frequency non-selective Rayleigh fading. Let h_{1r}, h_{2r}, h_{r1} and h_{r2} denote the fading coefficients for the following hops $S_1 \to R$, $S_2 \to R$, $R \to S_1$ and $R \to S_2$, respectively.[2] Similarly, let γ_{1r}, γ_{2r}, γ_{r1} and γ_{r2} denote the instantaneous SNRs for the links $S_1 \to R$, $S_2 \to R$, $R \to S_1$ and $R \to S_2$, respectively. To make the presentation simpler, we denote the instantaneous SNRs over different links by γ_{im} for $i = 1, 2$ and $m = 1, 2$ where $\gamma_{11} = \gamma_{1r}$, $\gamma_{12} = \gamma_{r2}$, $\gamma_{21} = \gamma_{2r}$ and $\gamma_{22} = \gamma_{r1}$, i.e., index i refers to the user and m refers to which hop of that user. To this end, the probability density function (pdf) of γ_{im} is given as

$$f_{\gamma_{im}}(\gamma_{im}) = \frac{1}{\overline{\gamma}_{im}} e^{-\frac{1}{\overline{\gamma}_{im}}\gamma_{im}}, \tag{1}$$

where $\overline{\gamma}_{im} = \rho E\left[|h_{im}|^2\right]$ is the average SNR for different links and $\rho = \frac{E_b}{N_0}$. For DF relaying, the E2E SNR of user i is approximated as $\gamma_i = \min(\gamma_{i1}, \gamma_{i2})$ [27], and its pdf is expressed as

$$f_{\gamma_i}(\gamma_i) = \frac{1}{\overline{\gamma}_i} e^{-\frac{1}{\overline{\gamma}_i}\gamma_i}, \tag{2}$$

where $\overline{\gamma}_i = \frac{\overline{\gamma}_{i1}\overline{\gamma}_{i2}}{\overline{\gamma}_{i1}+\overline{\gamma}_{i2}}$. Thus the E2E SNR of S_i in this paper refers to $\gamma_i = \min(\gamma_{i1}, \gamma_{i2})$.

III. Proposed Schemes

A. Hierarchical Zero Padding/Network Coding (HZPNC)

As mentioned above, this scheme involves using a 4/16-QAM hierarchical modulation, where one user uses 4-QAM and the other uses 16-QAM. Since the two user sequences received at the relay have different lengths, we use hierarchical zero padding with network coding. In the following subsections, we elaborate on how this scheme works.

1) Hierarchical 4/16-QAM: The 4/16 hierarchical constellation used in this paper is shown in Fig. 1. The filled circles represent the fictitious QPSK symbols and the blank circles represent the actual transmitted 16-QAM symbols. The transmitted bit sequence consists of two subsequences, HP bits and LP bits. The HP bits are assigned to the positions of the fictitious QPSK symbols, while the LP bits are assigned to the remaining positions. In the figure, $2d_1$ is the distance between two fictitious QPSK symbol points and $2d_2$ is the distance between the actual transmitted 16-QAM constellation points within one quadrant. The constellation priority parameter is denoted by $d = d_1/d_2$.

[2]The channel state information (CSI) is assumed to be perfectly known. Considering imperfect CSI is out of the scope of this paper. However, we believe that the conclusions made here still hold with imperfect CSI.

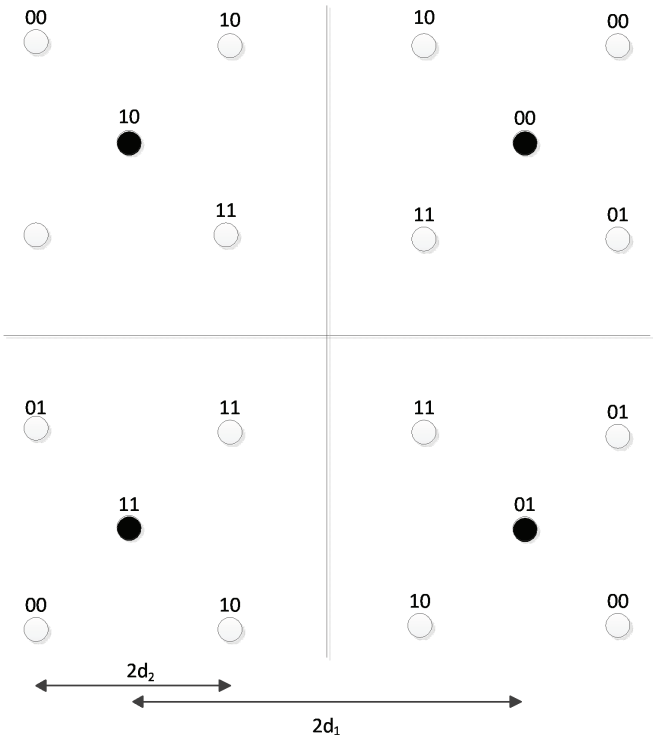

Fig. 1. 4/16-QAM hierarchical modulation.

2) Hierarchical Zero Padding: Since we assume that the two users have different data rates, the length of the bits sequences received from the two users at the relay will be different. In order to clearly illustrate the network coding schemes at the relay, we assume that the detected bit sequences from S_1 and S_2 at the relay are $\widehat{b}_1 = 1101$ and $\widehat{b}_2 = 11101011$, respectively. Conventional zero padding involves appending zeros to the end of $\widehat{b}_1$ to make it have the same length as that of $\widehat{b}_2$. Thus, $\widehat{b}_1 = 11010000$. Consequently, $\hat{b}_r = \widehat{b}_1 \oplus \widehat{b}_2 = 00111011$, which will then be modulated into a 16-QAM sequence and broadcasted to both users. In order to get their desired received data, both users need to decode these 16-QAM symbols.

For hierarchical zero padding, instead of adding zeros to the end of $\widehat{b}_1$, we append zeros to particular positions of $\widehat{b}_1$. Since 4/16-QAM hierarchical modulation is used at S_2, $\widehat{b}_2$ consists of HP bits ($\hat{b}_2^h = 1110$) and LP bits ($\hat{b}_2^l = 1011$). Note that the first two bits of every symbol are HP bits. At the relay, $\widehat{b}_1$ is XORed with $\hat{b}_2^h$ and the resulting bits are placed on the position of HP bits again. Then we get $\hat{b}_r^h = 0011$. The LP bits ($\hat{b}_2^l = 1011$) remain unchanged and placed on the LP bit positions, that is, $\hat{b}_r^l = 1011$. Then $\widehat{b}_r =$0$\underline{0}$10$\underline{1}\underline{1}$11 (the HP bits are underlined.) We can also understand this process in the following way. We treat the original bits of $\widehat{b}_1$ as HP bits, that is, $\hat{b}_1^h = 1101$. We put zeros on the position of LP bits of $\widehat{b}_1$, that is, $\hat{b}_1^l = 0000$. Then we get the new $\widehat{b}_1$ which is 11000100. Then $\widehat{b}_r = \widehat{b}_1 \oplus \widehat{b}_2 = 00101111$. $\widehat{b}_r$ is then modulated by the 4/16-QAM modulation and broadcasted to the two users. We can see that we put zeros on specific positions of $\widehat{b}_1$ to make it have the same length as $\widehat{b}_2$, hence the name hierarchical zero padding/network coding.

From the above description, the advantages of our proposed HZPNC scheme over original zero padding can be summarized as follows: 1) S_2 needs to only decode the fictitious 4-QAM symbols instead of decoding the 16-QAM symbols; 2) the E2E BER performance of S_1 is only influenced by the BER of the HP bits from S_2, which has better BER than that of the LP bits; and 3) According to 1) and 2), our proposed HZPNC scheme will have better E2E BER performance than that of the original zero padding for S_1, and this comes at no additional complexity.

3) Three time-slot DF Network Coding: Let y_{1r} and y_{2r} denote the signals received at the relay from S_1 and S_2, respectively (over two time-slots). These signals can be expressed as $y_{1r} = \sqrt{2\rho}h_{1r}x_1 + n_{1r}$ and $y_{2r} = \sqrt{4\rho}h_{2r}x_2 + n_{2r}$, where x_i $(i = 1, 2)$ denotes the transmitted signal from user i, and n_{ir} are additive white complex Gaussian noise (AWGN) samples with zero mean and unit variance. The relay then uses ML detection to detect the two signals (arriving from the two users over two time-slots). That is,

$$\begin{aligned}\hat{x}_1 &= \underset{x_1 \in 4-QAM}{\arg\min} \left| y_{1r} - \sqrt{2\rho}h_{1r}x_1 \right| \\ \hat{x}_2 &= \underset{x_2 \in 4/16-QAM}{\arg\min} \left| y_{2r} - \sqrt{4\rho}h_{2r}x_2 \right|.\end{aligned}$$

The resulting sequences are network-coded and modulated by 4/16-QAM modulation. The modulated signal x_r is broadcasted to both users in the third time-slot. The signals received at the two users are expressed as $y_{ri} = \sqrt{4\rho}h_{ri}x_r + n_{ri}$ $(i = 1, 2)$. Then the received signals can be decoded at the destination using ML as

$$\hat{x}_{r1} = \underset{x_r \in 16-QAM}{\arg\min} \left| y_{r_1} - \sqrt{4\rho}h_{r1}x_r \right|,$$

and

$$\hat{x}_{r2} = \underset{x_r \in fictitious\ 4-QAM}{\arg\min} \left| y_{r2} - \sqrt{4\rho}h_{r2}x_r \right|,$$

respectively. Note that the data of S_1 is embedded within the HP bits of x_r. As such, S_2 needs to only decode the HP bits which comprise the fictitious 4-QAM. Since each user knows its own transmitted signal, it can decode the desired signal according to the network coding scheme used at the relay.

B. Opportunistic User Selection (OUS)

For this scheme, only one user with the better E2E instantaneous SNR transmits at a time. That is, if $\gamma_i > \gamma_j$ $(i = 1, 2;\ j = 1, 2,$ s.t. $i \neq j)$, only user i transmits to user j with the help of the relay. Let us assume user 1 is selected as an example. In the first time slot, the selected user transmits to the relay, and the received signal at the relay is $y_r = \sqrt{2\rho}h_{1r}x_1 + n_{1r}$. Then the relay decodes the received signal as

$$\hat{x}_1 = \underset{x_1 \in 4-QAM}{\arg\min} \left| y_r - \sqrt{2\rho}h_{1r}x_1 \right|$$

The resulting sequence is modulated by 4-QAM modulation. The modulated signal x_r is transmitted to user 2. The signal received by user 2 is $y_2 = \sqrt{2\rho}h_{r2}x_r + n_{r2}$. Then this user can decode the received signal as

$$\hat{x}_r = \underset{x_r \in 4-QAM}{\arg\min} \left| y_2 - \sqrt{2\rho}h_{r2}x_r \right|.$$

IV. Bit Error Rate Performance Analysis

In this section, we derive closed-form expressions for E2E BER for the two relaying schemes, namely, HZPNC and OUS. For both schemes, we assume that S_1 employs 4-QAM and S_2 employs 4/16-QAM. However, the proposed schemes and performance analysis of these schemes can be extended to other hierarchical modulation schemes following the results of [28].

A. HZPNC Scheme

According to the proposed HZPNC, the bits from S_1 are XORed with the HP bits from S_2. Consequently, S_2 decodes only the fictitious 4-QAM constellation of the 4/16-QAM hierarchical constellation. The E2E BER at S_2 is given as [16]

$$\begin{aligned}P_{e,1} &= \left(1 - P_{e,r2}^{hp}\right) \left[\begin{array}{l} P_{e,1r}\left(1 - P_{e,2r}^{hp}\right) \\ +P_{e,2r}^{hp}\left(1 - P_{e,1r}\right) \end{array} \right] \\ &\quad + \left(1 - \left[\begin{array}{l} P_{e,1r}\left(1 - P_{e,2r}^{hp}\right) \\ +P_{e,2r}^{hp}\left(1 - P_{e,1r}\right) \end{array} \right] \right) P_{e,r2}^{hp}, \quad (3)\end{aligned}$$

where $P_{e,2r}^{hp}$ and $P_{e,r2}^{hp}$ are the probabilities of making an error over the $S_2 \to R$ and $R \to S_2$ links, respectively, for the HP bits from S_2; $P_{e,1r}$ is the BER over the $S_1 \to R$ link for the bits from S_1.

For the 4-QAM modulation, the BER over any of the links can be expressed as

$$P_{e,im} = \int_0^\infty P_e^{4QAM}(\gamma_{im}) f_{\gamma_{im}}(\gamma_{im})\, d\gamma_{im}, \quad (4)$$

where $P_e^{4QAM}(\gamma_{im})$ is the exact conditional BER, conditioned on the instantaneous SNR, and is given by

$$P_e^{4QAM}(\gamma_{im}) = \frac{1}{2}\operatorname{erf} c\sqrt{\gamma_{im}}, \quad (5)$$

and $f_{\gamma_{im}}(\gamma_{im})$ is expressed by (1).

Plugging (5) and (1) into (4) and carrying out the integration, we obtain

$$P_{e,im} = I_1\left(1, \overline{\gamma}_{im}\right), \quad (6)$$

where

$$\begin{aligned}I_1(a,b) &= \int_0^\infty \frac{1}{2}\operatorname{erf} c\sqrt{a\gamma_{im}}\frac{1}{b}e^{-\frac{1}{b}\gamma_{im}}d\gamma_{im} \\ &= \frac{1}{2}\left(1 - \sqrt{\frac{ab}{1+ab}}\right). \quad (7)\end{aligned}$$

Consequently, $P_{e,im}$ for the case $i = 1, m = 1$ ($S_1 \to R$ link) is given as $P_{e,1r} = I_1\left(1, \overline{\gamma}_{1r}\right)$.

In order to get the BER expression for S_2, we still need the BER expression for the HP bits for 4/16-QAM, which can be expressed as

$$P_{e,im}^{hp} = \int_0^\infty P_{e,hp}^{4/16QAM}(\gamma_{im}) f_{\gamma_{im}}(\gamma_{im})\, d\gamma_{im}, \quad (8)$$

where $P_{e,hp}^{4/16QAM}(\gamma_{im})$ is the exact conditional BER for the HP bits, conditioned on the instantaneous SNR for the 4/16-QAM modulation, and is given by [28]

$$P_{e,hp}^{4/16QAM}(\gamma_{im}) = \frac{1}{2}\left[\begin{array}{c} \frac{1}{2}\operatorname{erf} c\sqrt{\frac{2(d^2-2d+1)}{1+d^2}\gamma_{im}} \\ +\frac{1}{2}\operatorname{erf} c\sqrt{\frac{2(d^2+2d+1)}{1+d^2}\gamma_{im}} \end{array}\right], \quad (9)$$

where $d = d_1/d_2$ is the constellation priority parameter defined in Section II. Plugging (1) and (9) into (8) and carrying out the integration, we obtain

$$P_{e,im}^{hp} = \frac{1}{2}\left[\begin{array}{c} I_1\left(\frac{2(d^2-2d+1)}{1+d^2}, \overline{\gamma}_{im}\right) \\ +I_1\left(\frac{2(d^2+2d+1)}{1+d^2}, \overline{\gamma}_{im}\right) \end{array}\right]. \quad (10)$$

Note that $P_{e,2r}^{hp} = P_{e,21}^{hp}$ and $P_{e,r2}^{hp} = P_{e,12}^{hp}$. Plugging these expressions as well as that of $P_{e,1r}$ into (3) yields a closed-form expression for $P_{e,1}$.

Now for the BER at S_1, recall that the bits coming from S_2 consist of HP and LP bits. The HP bits are XORed with the bits from S_1 and the LP bits are relayed without network coding. As such, the E2E BER at S_1 is obtained as

$$P_{e,2} = \frac{1}{2}\left(P_{e,2}^{hp} + P_{e,2}^{lp}\right), \quad (11)$$

where $P_{e,2}^{hp}$ and $P_{e,2}^{lp}$ represent the E2E BER of the HP and LP bits, respectively. Now $P_{e,2}^{hp}$ can be expressed as [16]

$$\begin{aligned} P_{e,2}^{hp} &= \left(1-P_{e,r1}^{hp}\right)\left[\begin{array}{c} P_{e,1r}\left(1-P_{e,2r}^{hp}\right) \\ +P_{e,2r}^{hp}\left(1-P_{e,1r}\right) \end{array}\right] \\ &\quad + \left(1-\left[\begin{array}{c} P_{e,1r}\left(1-P_{e,2r}^{hp}\right) \\ +P_{e,2r}^{hp}\left(1-P_{e,1r}\right) \end{array}\right]\right) P_{e,r1}^{hp}, \quad (12) \end{aligned}$$

where $P_{e,1r}$ and $P_{e,2r}^{hp}$ are defined above. When $i = 2$, $m = 2$, we have $P_{e,r1}^{hp} = P_{e,22}^{hp}$. Having found expressions for all the terms in (12) ,we can easily find a closed-form expression for $P_{e,2}^{hp}$.

Concerning the LP bits, since they are relayed without network coding, the corresponding E2E BER is given by

$$P_{e,2}^{lp} = P_{e,2r}^{lp}(1-P_{e,r1}^{lp}) + (1-P_{e,2r}^{lp})P_{e,r1}^{lp}, \quad (13)$$

where

$$P_{e,im}^{lp} = \int_0^{\infty} P_{e,lp}^{4/16QAM}(\gamma_{im}) f_{\gamma_{im}}(\gamma_{im})\, d\gamma_{im}, \quad (14)$$

and $P_{e,lp}^{4/16QAM}(\gamma_{im})$ is the exact conditional BER for the LP bits conditioned on the instantaneous SNR for the 4/16-QAM modulation and is given by [28]

$$\begin{aligned} &P_{e,lp}^{4/16QAM}(\gamma_{im}) \\ &= \frac{1}{2}\left[\begin{array}{c} \operatorname{erf} c\sqrt{\frac{2}{1+d^2}\gamma_{im}} + \frac{1}{2}\operatorname{erf} c\sqrt{\frac{2(4d^2-4d+1)}{1+d^2}\gamma_{im}} \\ -\frac{1}{2}\operatorname{erf} c\sqrt{\frac{2(4d^2+4d+1)}{1+d^2}\gamma_{im}} \end{array}\right]. \end{aligned} \quad (15)$$

Plugging (1) and (15) into (14) and carrying out the integration, we obtain

$$\begin{aligned} P_{e,im}^{lp} &= I_1\left(\frac{2}{1+d^2}, \overline{\gamma}_{im}\right) \\ &\quad + \frac{1}{2}\left[\begin{array}{c} I_1\left(\frac{2(4d^2-4d+1)}{1+d^2}, \overline{\gamma}_{im}\right) \\ -I_1\left(\frac{2(4d^2+4d+1)}{1+d^2}, \overline{\gamma}_{im}\right) \end{array}\right]. \quad (16) \end{aligned}$$

By setting $i = 2$, $m = 2$ in (16), we obtain $P_{e,r1}^{lp} = P_{e,22}^{lp}$. We can similarly obtain $P_{e,1r}^{lp} = P_{e,11}^{lp}$. These expressions lead to a closed-form expression for $P_{e,2}^{lp}$. Having obtained expressions for $P_{e,2}^{hp}$ and $P_{e,2}^{lp}$, $P_{e,2}$ is obtained by plugging $P_{e,2}^{hp}$ and $P_{e,2}^{lp}$ into (11).

B. Original Zero Padding

We derive in this section the E2E BER performance of the original zero padding scheme, whereby the zeros are just added at the end of the shorter bit sequence. Recall that the bits from S_1 are XORed with the bits from S_2. Therefore, the E2E BER at S_2 can be expressed as

$$\begin{aligned} P_{e,1} &= (1-P_{e,r2})\left[\begin{array}{c} P_{e,1r}\left(1-P_{e,2r}\right) \\ +P_{e,2r}\left(1-P_{e,1r}\right) \end{array}\right] \\ &\quad + \left(1-\left[\begin{array}{c} P_{e,1r}\left(1-P_{e,2r}\right) \\ +P_{e,2r}\left(1-P_{e,1r}\right) \end{array}\right]\right) P_{e,r2}, \quad (17) \end{aligned}$$

where $P_{e,1r}$ is derived above. Since we do not distinguish between the HP and LP bits in the original zero padding scheme, the BER over different links is the same and can be expressed as

$$P_{e,im} = \frac{1}{2}\left(P_{e,im}^{hp} + P_{e,im}^{lp}\right), \quad (18)$$

where $P_{e,im}^{hp}$ and $P_{e,im}^{lp}$ are given in (10) and (16), respectively. Therefore, we have $P_{e,2r}^{hp} = P_{e,21}^{hp}$, $P_{e,r2}^{hp} = P_{e,22}^{hp}$, $P_{e,2r}^{lp} = P_{e,21}^{lp}$ and $P_{e,r2}^{lp} = P_{e,22}^{lp}$. Plugging the expressions for $P_{e,2r}^{hp}$ and $P_{e,2r}^{lp}$ into (18) yields an expression for $P_{e,2r}$. An expression for $P_{e,r2}$ can be obtained the same way. Plugging the expressions of $P_{e,1r}$, $P_{e,2r}$ and $P_{e,r2}$ into (17) yields an an expression for $P_{e,1}$.

Now we derive an expression for $P_{e,2}$. Note that half of the bits from S_2 are XORed with the bits coming from S_1, while the remaining bits are forwarded to the destination without network coding. Consequently, the E2E BER at S_1 can be expressed as

$$P_{e,2} = \frac{1}{2}(P_{e,2}^{NC} + P_{e,2}^{noNC}), \quad (19)$$

where

$$\begin{aligned} P_{e,2}^{NC} &= (1-P_{e,r1})\left[\begin{array}{c} P_{e,1r}\left(1-P_{e,2r}\right) \\ +P_{e,2r}\left(1-P_{e,1r}\right) \end{array}\right] \\ &\quad + \left(1-\left[\begin{array}{c} P_{e,1r}\left(1-P_{e,2r}\right) \\ +P_{e,2r}\left(1-P_{e,1r}\right) \end{array}\right]\right) P_{e,r1} \quad (20) \end{aligned}$$

and

$$P_{e,2}^{noNC} = P_{e,2r}(1-P_{e,r1}) + (1-P_{e,2r})P_{e,r1}. \quad (21)$$

From (18), we can obtain an expression for $P_{e,r1}$. By plugging the expression of $P_{e,r1}$, $P_{e,2r}$ and $P_{e,1r}$ into (20) and (21), we can get expressions for $P_{e,2}^{NC}$ and $P_{e,2}^{noNC}$.

C. OUS Scheme

For this scheme, if the instantaneous E2E SNR of S_i is greater than that of S_j, only S_i transmits to S_j. Thus, when either the $S_i \to R$ or $R \to S_j$ link is in error, the received signal at S_j will be in error. Therefore, the E2E BER of S_i can be expressed as

$$\begin{aligned} & P(\varepsilon_i \,|\gamma_i > \gamma_j\,) \\ = \;& P(\varepsilon_{im}\,|\gamma_i > \gamma_j\,)(1 - P(\varepsilon_{in}\,|\gamma_i > \gamma_j\,)) \\ & + P(\varepsilon_{in}\,|\gamma_i > \gamma_j\,)(1 - P(\varepsilon_{im}\,|\gamma_i > \gamma_j\,)), \end{aligned} \quad (22)$$

where $i, j = 1, 2$, with $i \neq j$, and $m, n = 1, 2$, with $m \neq n$. The indices have the same definition as that of γ_{im} in Section II, that is, $P(\varepsilon_{11}\,|\gamma_1 > \gamma_2\,)$ refers to $P(\varepsilon_{1r}\,|\gamma_1 > \gamma_2\,)$, which represents the BER over the $S_1 \to R$ link given that $\gamma_1 > \gamma_2$. Since S_1 employs 4-QAM, the BER over different links can be expressed as

$$P(\varepsilon_{1m}\,|\gamma_1 > \gamma_2\,) = \int_0^\infty P_e^{4QAM}(\gamma_{1m}) f_{\gamma_{1m}|\gamma_1>\gamma_2}(\gamma_{1m}) d\gamma_{1m}\,. \quad (23)$$

The pdf of γ_{im} conditioned on $\gamma_i > \gamma_j$ is derived as (see Appendix)

$$\begin{aligned} f_{\gamma_{im}|\gamma_i>\gamma_j}(\gamma_{im}) = & \frac{\overline{\gamma}_{in}(\overline{\gamma}_i + \overline{\gamma}_j)}{\overline{\gamma}_{im}\overline{\gamma}_i(\overline{\gamma}_{in} + \overline{\gamma}_j)} \\ & \cdot \left(e^{-\frac{1}{\overline{\gamma}_{im}}\gamma_{im}} - e^{-(\frac{1}{\overline{\gamma}_i} + \frac{1}{\overline{\gamma}_j})\gamma_{im}} \right). \end{aligned} \quad (24)$$

Plugging (5) and (24) into (23) and carrying out the integration, we obtain

$$\begin{aligned} P(\varepsilon_{1m}\,|\gamma_1 > \gamma_2\,) = & \frac{\overline{\gamma}_{1n}(\overline{\gamma}_1 + \overline{\gamma}_2)}{\overline{\gamma}_{1m}\overline{\gamma}_1(\overline{\gamma}_{1n} + \overline{\gamma}_2)} \\ & \cdot \begin{bmatrix} \overline{\gamma}_{1m} I_1\,(1, \overline{\gamma}_{1m}) \\ -\frac{\overline{\gamma}_1\overline{\gamma}_2}{\overline{\gamma}_1+\overline{\gamma}_2} I_1\left(1, \frac{\overline{\gamma}_1\overline{\gamma}_2}{\overline{\gamma}_1+\overline{\gamma}_2}\right) \end{bmatrix}. \end{aligned} \quad (25)$$

Note that $P(\varepsilon_{1r}\,|\gamma_1 > \gamma_2\,) = P(\varepsilon_{22}\,|\gamma_1 > \gamma_2\,)$ and $P(\varepsilon_{r2}\,|\gamma_1 > \gamma_2\,) = P(\varepsilon_{12}\,|\gamma_1 > \gamma_2\,)$. Plugging these expressions into (22) yields a closed from expression for $P(\varepsilon_1\,|\gamma_1 > \gamma_2\,)$.

Since S_2 uses hierarchical 4/16-QAM modulation and we do not distinguish between the HP and LP bits, $P(\varepsilon_{2m}\,|\gamma_2 > \gamma_1\,)$ is given by

$$P(\varepsilon_{2m}\,|\gamma_2 > \gamma_1\,) = \frac{1}{2}(P(\varepsilon_{2m}^{hp}\,|\gamma_2 > \gamma_1\,) + P(\varepsilon_{2m}^{lp}\,|\gamma_2 > \gamma_1\,)), \quad (26)$$

where $P(\varepsilon_{2m}^{hp}\,|\gamma_2 > \gamma_1\,)$ represents the BER of the HP bits given that $\gamma_2 > \gamma_1$, and $P(\varepsilon_{2m}^{lp}\,|\gamma_2 > \gamma_1\,)$ represents the BER of the LP bits given that $\gamma_2 > \gamma_1$. The BER of the HP bits can be expressed as

$$P(\varepsilon_{2m}^{hp}\,|\gamma_2 > \gamma_1\,) = \int_0^\infty P_{e,hp}^{4/16QAM}(\gamma_{2m}) f_{\gamma_{2m}|\gamma_2>\gamma_1}(\gamma_{2m}) d\gamma_{2m}\,. \quad (27)$$

Plugging (9) and (24) into (27) and carrying out the integration, we obtain

$$\begin{aligned} P(\varepsilon_{2m}^{hp}\,|\gamma_2 > \gamma_1\,) = & \frac{1}{2}\frac{\overline{\gamma}_{2n}(\overline{\gamma}_1 + \overline{\gamma}_2)}{\overline{\gamma}_{2m}\overline{\gamma}_2(\overline{\gamma}_{2n} + \overline{\gamma}_1)} \\ & \cdot \left\{ \begin{array}{c} \overline{\gamma}_{2m} \left[\begin{array}{c} I_1\left(\frac{2(d^2-2d+1)}{1+d^2}, \overline{\gamma}_{2m}\right) \\ +I_1\left(\frac{2(d^2+2d+1)}{1+d^2}, \overline{\gamma}_{2m}\right) \end{array} \right] \\ -\frac{\overline{\gamma}_1\overline{\gamma}_2}{\overline{\gamma}_1+\overline{\gamma}_2} \left[\begin{array}{c} I_1\left(\frac{2(d^2-2d+1)}{1+d^2}, \frac{\overline{\gamma}_1\overline{\gamma}_2}{\overline{\gamma}_1+\overline{\gamma}_2}\right) \\ +I_1\left(\frac{2(d^2+2d+1)}{1+d^2}, \frac{\overline{\gamma}_1\overline{\gamma}_2}{\overline{\gamma}_1+\overline{\gamma}_2}\right) \end{array} \right] \end{array} \right\}. \end{aligned} \quad (28)$$

Note that $P(\varepsilon_{2r}^{hp}\,|\gamma_2 > \gamma_1\,) = P(\varepsilon_{22}^{hp}\,|\gamma_2 > \gamma_1\,)$ and $P(\varepsilon_{r1}^{hp}\,|\gamma_2 > \gamma_1\,) = P(\varepsilon_{21}^{hp}\,|\gamma_2 > \gamma_1\,)$.

Similarly, the BER of the LP bits can be expressed as

$$P(\varepsilon_{2m}^{lp}\,|\gamma_2 > \gamma_1\,) = \int_0^\infty P_{e,lp}^{4/16QAM}(\gamma_{2m}) f_{\gamma_{2m}|\gamma_2>\gamma_1}(\gamma_{2m}) d\gamma_{2m}\,. \quad (29)$$

Then plugging (15) and (24) into (29) and carrying out the integration, we obtain

$$\begin{aligned} P(\varepsilon_{2m}^{lp}\,|\gamma_2 > \gamma_1\,) = & \frac{\overline{\gamma}_{2n}(\overline{\gamma}_2 + \overline{\gamma}_1)}{\overline{\gamma}_{2m}\overline{\gamma}_2(\overline{\gamma}_{2n} + \overline{\gamma}_1)} \\ & \cdot \left\{ \begin{array}{c} \overline{\gamma}_{2m} \left[\begin{array}{c} I_1\left(\frac{2}{1+d^2}, \overline{\gamma}_{2m}\right) \\ +\frac{1}{2}I_1\left(\frac{2(4d^2-4d+1)}{1+d^2}, \overline{\gamma}_{2m}\right) \\ -\frac{1}{2}I_1\left(\frac{2(4d^2+4d+1)}{1+d^2}, \overline{\gamma}_{2m}\right) \end{array} \right] \\ -\frac{\overline{\gamma}_1\overline{\gamma}_2}{\overline{\gamma}_1+\overline{\gamma}_2} \left[\begin{array}{c} I_1\left(\frac{2}{1+d^2}, \frac{\overline{\gamma}_1\overline{\gamma}_2}{\overline{\gamma}_1+\overline{\gamma}_2}\right) \\ +\frac{1}{2}I_1\left(\frac{2(4d^2-4d+1)}{1+d^2}, \frac{\overline{\gamma}_1\overline{\gamma}_2}{\overline{\gamma}_1+\overline{\gamma}_2}\right) \\ -\frac{1}{2}I_1\left(\frac{2(4d^2+4d+1)}{1+d^2}, \frac{\overline{\gamma}_1\overline{\gamma}_2}{\overline{\gamma}_1+\overline{\gamma}_2}\right) \end{array} \right] \end{array} \right\}. \end{aligned} \quad (30)$$

Note that $P(\varepsilon_{2r}^{lp}\,|\gamma_2 > \gamma_1\,) = P(\varepsilon_{21}^{lp}\,|\gamma_2 > \gamma_1\,)$ and $P(\varepsilon_{r1}^{lp}\gamma_2 > \gamma_1) = P(\varepsilon_{22}^{lp}\,|\gamma_2 > \gamma_1\,)$.

Having obtained the expressions for $P(\varepsilon_{2m}^{hp}\,|\gamma_2 > \gamma_1\,)$ and $P(\varepsilon_{2m}^{lp}\,|\gamma_2 > \gamma_1\,)$, $P(\varepsilon_{2r}\,|\gamma_2 > \gamma_1\,)$ is obtained by plugging $P(\varepsilon_{2r}^{hp}\,|\gamma_2 > \gamma_1\,)$ and $P(\varepsilon_{2r}^{lp}\,|\gamma_2 > \gamma_1\,)$ into (26) and $P(\varepsilon_{r1}\,|\gamma_2 > \gamma_1\,)$ is obtained by plugging $P(\varepsilon_{r1}^{hp}\,|\gamma_2 > \gamma_1\,)$ and $P(\varepsilon_{r1}^{lp}\,|\gamma_2 > \gamma_1\,)$ into (26). Plugging the derived expressions $P(\varepsilon_{2r}\,|\gamma_2 > \gamma_1\,)$ and $P(\varepsilon_{r1}\,|\gamma_2 > \gamma_1\,)$ into (22), we obtain a closed-form expression for $P(\varepsilon_2\,|\gamma_2 > \gamma_1\,)$, as desired.

V. Access Probability and Throughput Analysis

In this section, we compare the HZPNC and OUS schemes in terms of access probability and throughput.

A. Access Probability

According to the HZPNC scheme, both users transmit via channel sharing. The two users communicate with each other over three time-slots. During the three time-slots, each user occupies two time-slots with one time-slot overlapping. Therefore, the access probability for both users is

$$P_i^{HZPNC} = \frac{2}{3}. \quad (31)$$

As for the OUS scheme, a user transmits once its instantaneous E2E SNR is greater than that of the other one, resulting in an

access probability of

$$\begin{aligned} P_i^{OUS} &= P_r(\gamma_i > \gamma_j) \\ &= \int_0^{\infty} \frac{1}{\overline{\gamma}_j} e^{-\frac{\gamma_j}{\overline{\gamma}_j}} dz_j \int_{\gamma_j}^{\infty} \frac{1}{\overline{\gamma}_i} e^{-\frac{\gamma_i}{\overline{\gamma}_i}} d\gamma_1 \\ &= \frac{\overline{\gamma}_i}{\overline{\gamma}_i + \overline{\gamma}_j} \qquad (32) \\ &\triangleq \frac{k_i}{k_i + 1}, \qquad (33) \end{aligned}$$

where $k_i \triangleq \overline{\gamma}_i/\overline{\gamma}_j$. From (33), we observe that P_i^{OUS} only depends on the value of k_i. For symmetric channels, for example, the average E2E SNRs are the same, i.e., $k_i = 1$, suggesting that both users will have the same access probability, which is $P_i^{OUS} = 0.5$. In this case, the OUS scheme has a lower access probability compared to that of the HZPNC scheme for each user by $\frac{1}{6}$.

Now define $\triangle P_i$ as

$$\begin{aligned} \triangle P_i &\triangleq P_i^{HZPNC} - P_i^{OUS} \\ &= \frac{2}{3} - \frac{k_i}{k_i + 1}, \qquad (34) \end{aligned}$$

which represents the access probability difference between the two schemes. Solving $\frac{2}{3} - \frac{k_i}{k_i+1} > 0$, we obtain $\frac{1}{2} < k_i < 2$, which is the range of k_i for which the HZPNC scheme has a higher access probability than that of the OUS scheme for both users. Beyond this range, one user of the OUS scheme will have a higher access probability than those of the HZPNC scheme, whereas the other one will have a lower access probability.

B. Throughput

We do the throughput analysis for the general case where it is assumed that S_1 uses 2^{2s}-QAM and S_2 uses $2^{2s}/2^{2r}$-QAM hierarchical modulation for $s = 1, 2, \ldots, r-1$, and $r = 2, 3, \ldots, R$. Since three time-slots are used for HZPNC, the corresponding throughput can be expressed as

$$T^{HZPNC} = \frac{2(s+r)}{3}, \qquad (35)$$

whereas for OUS, when a user transmits, it needs two time-slots to finish its transmission, thus the corresponding throughput is expressed as

$$T^{OUS} = \frac{2s \times P_r(\gamma_1 > \gamma_2) + 2r \times P_r(\gamma_2 > \gamma_1)}{2}. \qquad (36)$$

Plugging (32) into (36), we obtain

$$\begin{aligned} T^{OUS} &= \frac{s\overline{\gamma}_1 + r\overline{\gamma}_2}{\overline{\gamma}_1 + \overline{\gamma}_2} \\ &= \frac{sk_1 + r}{k_1 + 1}, \qquad (37) \end{aligned}$$

where k_1 is defined above. Now define $\triangle T$ as

$$\begin{aligned} \triangle T &\triangleq T^{HZPNC} - T^{OUS} \\ &= \frac{2(s+r)}{3} - \frac{sk_1 + r}{k_1 + 1}, \qquad (38) \end{aligned}$$

which is the throughput difference between the two schemes.

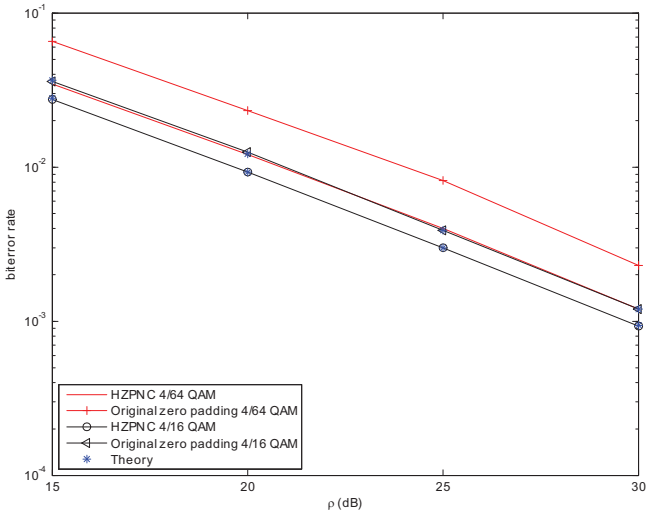

Fig. 2. E2E BER performance of the original zero padding and HZPNC schemes (for S_1).

For symmetric channels, i.e., $k_1 = 1$, we have $\triangle T = \frac{s+r}{6}$, suggesting that HZPNC achieves a higher throughput, as expected. However, it is not straightforward to say which scheme has a higher throughput for asymmetric channels, that is, when $k_1 \neq 1$. For fixed values of s and r, $\triangle T$ is only a function of k_1. We can consider two cases as examples. One is the example used throughout this paper where $s = 1$ and $r = 2$. Plugging $s = 1$ and $r = 2$ into (38), we obtain $\triangle T = \frac{k_1}{k_1+1}$, suggesting that T^{HZPNC} is greater than T^{OUS} by $\frac{k_1}{k_1+1}$.

Another example is when $s = 1$ and $r = 4$, which corresponds to S_1 using 4-QAM and S_2 using 4/256-QAM hierarchical modulation. Plugging $s = 1$ and $r = 4$ into (38), we obtain $\triangle T = \frac{7k_1-2}{3(k_1+1)}$. By solving $\frac{7k_1-2}{3(k_1+1)} > 0$, we find that $\triangle T > 0$ when $k_1 > \frac{2}{7}$, meaning that T^{HZPNC} is greater than T^{OUS} by $\frac{7k_1-2}{3(k_1+1)}$ for $k_1 > \frac{2}{7}$. On the other hand, $T^{NC} < T^{OUS}$ by $\frac{7k_1-2}{3(k_1+1)}$ when $k_1 < \frac{2}{7}$. Nonetheless, the probability that T^{NC} is less than T^{OUS} is very small, and it happens only when one user has a much higher modulation and access probability than those of the other user.

VI. Simulation Results

We present in this section numerical examples that aim at validating the E2E BER expressions derived for HZPNC and OUS. We also study the impact of varying the priority parameter d on the BER performance of HZPNC. In addition, we compare the two schemes in terms of E2E BER, access probability and throughput. Throughout the simulations, we assume that S_1 uses 4-QAM and S_2 uses 4/16-QAM hierarchical modulation, $d = 2$ and all channel variances are set to one, unless mentioned otherwise.

In Fig. 2, we compare the simulated E2E BER and the theoretical one based on the expressions derived in Section IV for the original zero padding and HZPNC schemes (for S_1). We also plot the simulation results for the case when S_1 uses 4-QAM and S_2 uses 4/64-QAM. As shown in the figure, the simulation results agree with the theoretical results.

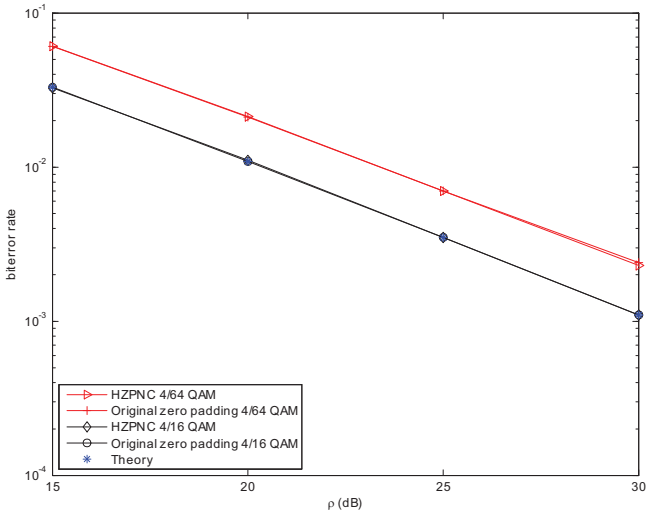

Fig. 3. E2E BER performance of the original zero padding and HZPNC schemes (for S_2).

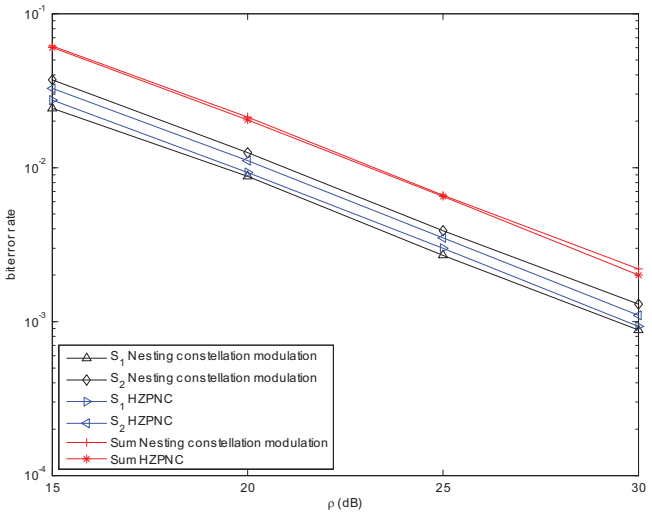

Fig. 5. Comparision of E2E BRR performance of Nesting constellation modulation and HZPNC.

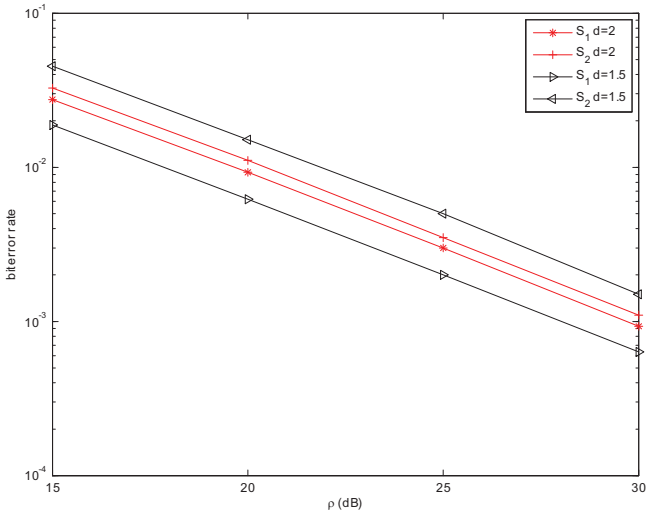

Fig. 4. Effect of variation of d on the E2E BER performance for two users.

We also observe the superiority of HZPNC over the original zero padding scheme for S_1, which is about 1 dB for 4/16-QAM and 3 dB for 4/64-QAM, and this comes at no additional complexity. This improvement is attributed to the fact that S_2 needs only to decode the fictitious 4-QAM instead of 16-QAM, and the E2E BER performance is only influenced by the BER of the HP bits from S_2, which have a lower BER than that of the LP bits. The results for S_2 are reported in Fig. 3. We also observe from the figure the perfect match between theory and simulations. In addition, our proposed HZPNC scheme achieves the same performance as the original zero padding for S_2.

In Fig. 4, we examine the influence of the value of d on the BER performance of the two users. We consider two values of d, namely 1.5 and 2. We observe from the figure that the performance of S_1 improves as d decreases from 2 to 1.5, whereas the performance of S_2 deteriorates. The improvement in the performance of S_1 is due to the fact that the BER of the HP bits is improved as d decreases, and this comes at the expense of deteriorating the BER of the LP bits. The consequence of this is a deterioration of the BER performance of S_2 since it depends on the LP bits. So the conclusion here is that changing the value of d improves the performance of one user while it deteriorates the performance of the other.

In Fig. 5, we compare the E2E BER performance of HZPNC against that of the nesting constellation modulation proposed in [20]. For nesting constellation modulation, the sequence length mismatch at the relay is taken care of by using repetition coding. For example, let $\widehat{b}_1 = 1101$. Then it is encoded into $\widehat{b}_1 = 11110011$, which now has the same length as that of $\widehat{b}_2 = 11101011$. Then $\widehat{b}_r = \widehat{b}_1 \oplus \widehat{b}_2 = 00101111$ is modulated as 16-QAM and broadcasted to the destinations. For S_2 to recover the signal of interest, it needs to do a constellation conversion from 16-QAM to 4-QAM according to Table I in [20]. As shown in the figure, the performance of S_1 is slightly better than that of HZPNC and the performance of S_2 is the opposite. As a whole, both schemes almost have similar sum BER performance (the average performance of both users), except that the nesting constellation modulation is more complex.

In Fig. 6, we compare the E2E BER performance of HZPNC with that of superposition modulation [6]. For the latter scheme, after the relay decodes the 4-QAM symbol $\hat{x}_1$ from S_1 and the 16-QAM symbol $\hat{x}_2$ from S_2, it divides its power between these two symbols and transmits $\hat{x}_r = \sqrt{1-\gamma^2}\hat{x}_1 + \sqrt{\gamma^2}\hat{x}_2$ to the destinations. Then a destination subtracts its own symbol and decodes the desired signal. In the simulations, we set $\gamma = 0.8$, $\gamma = 0.5$ and $\gamma = 0.2$. It is shown in the figure that the performance of HZPNC is better than that of superposition modulation, and the gap increases as γ decreases. We remark that the plotted performance is the average of the performance of the two users.

We compare in Fig. 7 the BER performance of HZPNC and OUS for S_1. For presentation convenience, we let the set $\{E\left[|h_{1r}|^2\right], E\left[|h_{2r}|^2\right], E\left[|h_{r2}|^2\right], E\left[|h_{r1}|^2\right]\}$ denote

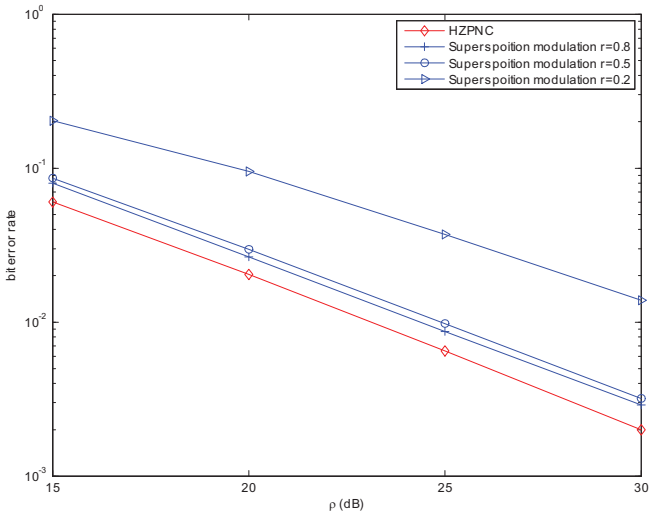

Fig. 6. Comparision of the sum BER performance of Superposition modulation and HZPNC.

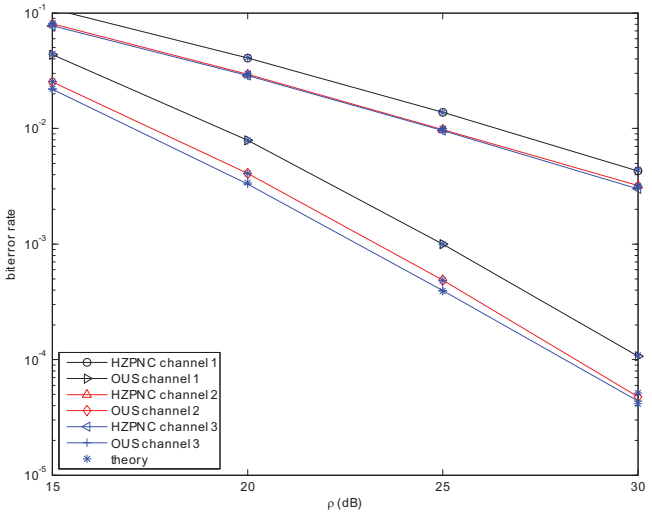

Fig. 8. Bit error rate performance (simulated and theoretical) of HZPNC and OUS for S_2.

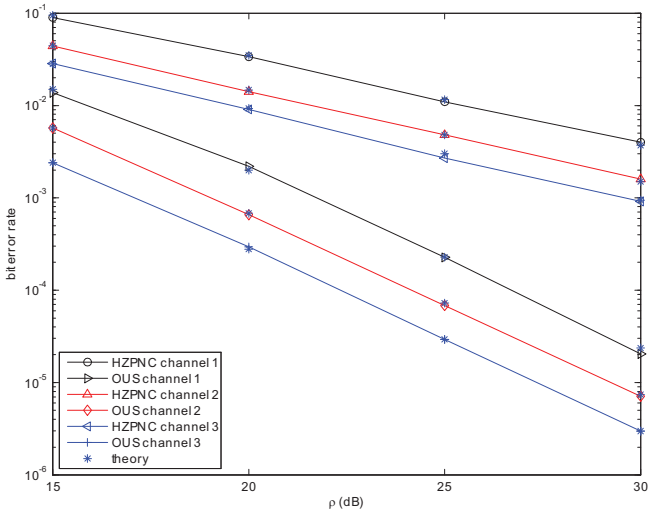

Fig. 7. Bit error rate performance (simulated and theoretical) of HZPNC and OUS for S_1.

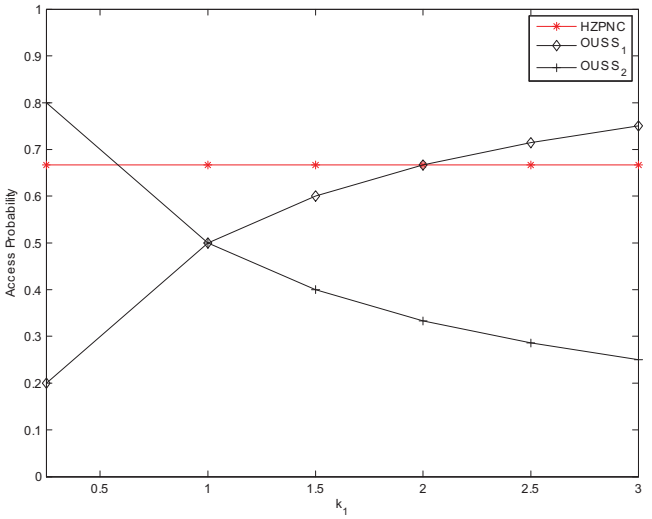

Fig. 9. Access probability for HZPNC and OUS.

the variances of the four subchannels. In the simulations, for both schemes, we randomly set channel 1 as $\left(\frac{1}{4},\ \frac{1}{4},\ \frac{1}{4},\ \frac{1}{4}\right)$, channel 2 as $\left(\frac{1}{2},\ 1,\ \frac{1}{2},\ \frac{1}{5}\right)$, and channel 3 as $\left(1,\ 1,\ 1,\ \frac{1}{5}\right)$. From the figure, we observe the following. First, there is a perfect match between simulations and theory, which validates our analysis. Second, it is shown that HZPNC achieves diversity order one, while OUS achieves diversity order two, which is expected since OUS benefits from the multiuser diversity gain. Finally, it is shown that OUS has a better E2E BER performance than that of HZPNC for all channels. The E2E BER performance for S_2 is shown in Fig. 8, with similar observations. However, the performance superiority of OUS over HZPNC comes at the expense of much reduced throughput, as will be demonstrated below.

In Fig. 9, we show the access probability for different values of k_1 for HZPNC and OUS. The access probability of HZPNC remains unchanged during all the range, which is $\frac{2}{3}$. Whereas, for OUS, when $\overline{\gamma}_1 < \overline{\gamma}_2$, S_1 has a lower access probability than S_2. The opposite is true when $\overline{\gamma}_1 > \overline{\gamma}_2$, which is expected. It is also shown that both OUS users have a lower access probability than the HZPNC users for the range $\frac{1}{2} < k_1 < 2$. While for the range $k_1 > 2$, S_1 has a higher access probability and S_2 has a lower access probability than those for HZPNC. However, for $k_1 < \frac{1}{2}$, the two OUS users exchange roles. For $k_1 = 1$, both users have the same chance to access the channel. For this case, the access probability is $\frac{1}{2}$ for both users which is $\frac{1}{6}$ less than that of the HZPNC scheme.

In Fig. 10, we show the throughput for different values of k_1 for both HZPNC and OUS. We consider two cases. In both cases, S_1 uses 4-QAM, whereas S_2 uses 4/16-QAM or 4/256-QAM. For all scenarios, we find that the throughput of OUS decreases with increasing k_1. This is expected since S_1 uses a lower order modulation scheme than that of S_2. Obviously if S_1 has a better chance to transmit, the average throughput will decrease. In addition, if S_2 employs 4/16-QAM, the throughput of HZPNC will always be higher than that of OUS.

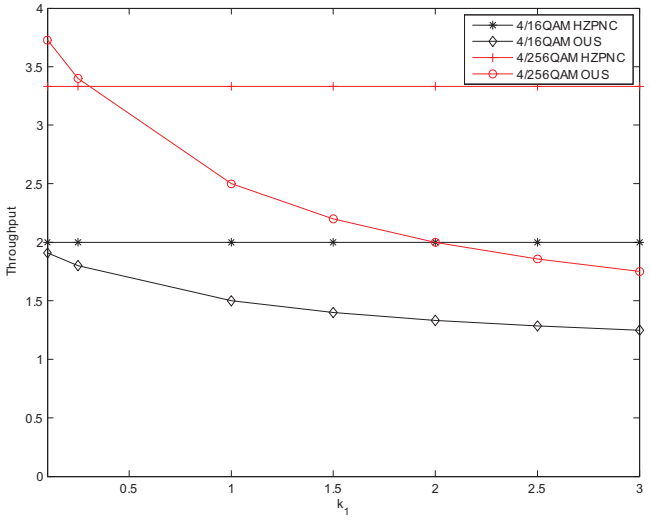

Fig. 10. Throughput for HZPNC and OUS.

However, if S_2 uses a much higher modulation scheme such as 4/256-QAM and this user also has a much higher access probability, the throughput of OUS will be higher than that of HZPNC, which is illustrated in the figure.

VII. Concluding Remarks

We have studied in this paper two DF relaying schemes for two-way relay channels with asymmetric data rates, namely HZPNC and OUS. We analyzed both schemes where we derived closed-form expressions for the E2E BER performance. We also studied both schemes in terms of the access probability and throughput. We showed that each scheme offers certain advantages over the other. For instance, the HZPNC scheme offers better throughput, but this comes at the expense of degraded E2E BER performance as compared to that of OUS. On the other hand, the OUS scheme achieves better E2E BER performance, taking advantage of the multiuser diversity. The pitfall of OUS, however, is the lack of fairness between the communicating users. That is, depending on the individual channel quality, one user may enjoy better access probability than the other. We also compared the performance of HZPNC with existing schemes, including the original zero padding, nesting constellation modulation and superposition modulation. We demonstrated the efficacy of the HZPNC scheme over all schemes in terms of the BER performance and/or complexity. Since these two schemes offer different advantages, it is natural to devise a hybrid scheme that combines these two schemes. This will be considered in a future work.

Proof of Equation (24)

The pdf of γ_{im} given $\gamma_i > \gamma_j$ can be expressed as

$$f_{\gamma_{im}|\gamma_i>\gamma_j}(\gamma_{im}) = \int_0^\infty f_{\gamma_{im}|\gamma_i=\gamma}(\gamma_{im})\, f_{\gamma_i|\gamma_i>\gamma_j}(\gamma) d\gamma, \quad (39)$$

where $\gamma_i = \min(\gamma_{im}, \gamma_{in})$ for $i, j, n, m = 1, 2$ where $i \neq j$, and $m \neq n$. The pdf of γ_{im} and γ_i is given in (1) and (2). Thus (44) can be further expressed as [29]

$$f_{\gamma_{im}|\gamma_i>\gamma_j}(\gamma_{im}) = \int_0^\infty \frac{\frac{1}{\overline{\gamma}_{im}} e^{-\frac{\gamma_{im}}{\overline{\gamma}_{im}}} \frac{1}{\overline{\gamma}_{in}} e^{-\frac{\gamma_{in}}{\overline{\gamma}_{in}}}}{\frac{1}{\overline{\gamma}_i} e^{-\frac{\gamma_i}{\overline{\gamma}_i}}} f_{\gamma_i|\gamma_i>\gamma_j}(\gamma) d\gamma + \frac{\frac{1}{\overline{\gamma}_{im}} e^{-\frac{\gamma_{im}}{\overline{\gamma}_{im}}} e^{-\frac{\gamma_{in}}{\overline{\gamma}_{in}}}}{\frac{1}{\overline{\gamma}_i} e^{-\frac{\gamma_{im}}{\overline{\gamma}_i}}} f_{\gamma_i|\gamma_i>\gamma_j}(\gamma_{im}), \quad (40)$$

where $i, j, n, m = 1, 2$, and $i \neq j, m \neq n$. The conditional cumulative distribution function (CDF) $F(\gamma_i \,|\gamma_i > \gamma_j)$ can be expressed as

$$F_{\gamma_i|\gamma_i>\gamma_j}(\gamma) = \frac{P_r(\gamma_i < \gamma,\ \gamma_i > \gamma_j)}{P_r(\gamma_i > \gamma_j)}. \quad (41)$$

By using the law of total probability, the numerator in (41) is given by

$$P_r(\gamma_i < \gamma, \gamma_i > \gamma_j) = \int_0^\gamma \frac{1}{\overline{\gamma}_i} e^{-\frac{\gamma_i}{\overline{\gamma}_i}} d\gamma_i \int_0^{\gamma_i} \frac{1}{\overline{\gamma}_j} e^{-\frac{\gamma_j}{\overline{\gamma}_j}} d\gamma_j = 1 - e^{-\frac{\gamma}{\overline{\gamma}_i}} - \frac{1}{\overline{\gamma}_i} \frac{1}{\frac{1}{\overline{\gamma}_i} + \frac{1}{\overline{\gamma}_j}} \left(1 - e^{-(\frac{1}{\overline{\gamma}_i} + \frac{1}{\overline{\gamma}_j})\gamma}\right), \quad (42)$$

and the denominator is given by

$$P_r(\gamma_i > \gamma_j) = \int_0^\infty \frac{1}{\overline{\gamma}_j} e^{-\frac{\gamma_j}{\overline{\gamma}_j}} dz_j \int_{\gamma_j}^\infty \frac{1}{\overline{\gamma}_i} e^{-\frac{\gamma_i}{\overline{\gamma}_i}} d\gamma_1 = \frac{\overline{\gamma}_i}{\overline{\gamma}_i + \overline{\gamma}_j}. \quad (43)$$

Plugging (42) and (43) into (41), we can derive the conditional CDF $F_{\gamma_i|\gamma_i>\gamma_j}(\gamma)$. The conditional pdf $f_{\gamma_i|\gamma_i>\gamma_j}(\gamma)$ is obtained by taking the derivative of $F_{\gamma_i|\gamma_i>\gamma_j}(\gamma)$ as

$$f_{\gamma_i|\gamma_i>\gamma_j}(\gamma) = \frac{\overline{\gamma}_i + \overline{\gamma}_j}{\overline{\gamma}_i} \left[\frac{1}{\overline{\gamma}_i} e^{-\frac{\gamma}{\overline{\gamma}_i}} - \frac{1}{\overline{\gamma}_i} e^{-(\frac{1}{\overline{\gamma}_i} + \frac{1}{\overline{\gamma}_j})\gamma}\right]. \quad (44)$$

Plugging (44) into (40) and carrying out the integration, we can get

$$f_{\gamma_{im}|\gamma_i>\gamma_j}(\gamma_{im}) = \frac{\overline{\gamma}_{in}(\overline{\gamma}_i + \overline{\gamma}_j)}{\overline{\gamma}_{im}\overline{\gamma}_i(\overline{\gamma}_{in} + \overline{\gamma}_j)} \cdot \left(e^{-\frac{1}{\overline{\gamma}_{im}}\gamma_{im}} - e^{-(\frac{1}{\overline{\gamma}_i} + \frac{1}{\overline{\gamma}_j})\gamma_{im}}\right), \quad (45)$$

where $i, j, n, m = 1, 2$ and $i \neq j, m \neq n$.

References

[1] A. Sendonaris, E. Erkip, and B. Aazhang, "User cooperation diversity—part I: system description," *IEEE Trans. Commun.*, vol. 51, pp. 1927–1938, Nov. 2003.

[2] A. Sendonaris, E. Erkip, and B. Aazhang, "User cooperation diversity—part II: implement aspects and performance analysis," *IEEE Trans. Commun.*, vol. 51, pp. 1927–1938, Nov. 2003.

[3] J. N. Laneman, D. N. C. Tse, and G. W. Wornell, "Cooperative diversity in wireless networks: efficient protocols and outage behavior," *IEEE Trans. Inf. Theory*, vol. 50, pp. 3062–3080, Dec. 2004.

[4] R. Ahlswede, N. Cai, S.-Y. R. Li, and R. W. Yeung, "Network information flow," *IEEE Trans. Inf. Theory*, vol. IT-46, pp. 1204–1216, July 2000.

[5] T. Wang and G. B. Giannakis, "Complex field network coding for multiuser cooperative communications," *IEEE J. Sel. Areas Commun.*, vol. 26, no. 3, pp. 561–571, Apr. 2008.

[6] Y. Hu, K. H. Li, and K. C. Teh, "Performance analysis of two-user multiple access systems with DF relaying and superposition modulation," *IEEE Trans. Veh. Technol.*, vol. 60, pp. 3118–3126, Sep. 2011.

[7] H. V. Nguyen, C. Xu, S. X. Ng, and L. Hanzo, "Non-coherent near-capacity network coding for cooperative multi-user communications," *IEEE Trans. Commun.*, vol. 60, no. 10, pp. 3059–3070, Oct. 2012.

[8] S. Katti, S. S. Gollakota, and D. Katabi, "Embracing wireless interference: analog network coding," MIT Tech. Report, Cambridge, Ma, Feb. 2007.

[9] K.-S. Hwang, Y.-C. Ko, and M.-S. Alouini, "Performance bounds for two-way amplify-and-forward relaying based on relay path selection," in *Proc. 2009 IEEE VTC – Spring*.

[10] K.-S. Hwang, Y.-C. Ko, and M.-S. Alouini, "Performance analysis of two-way amplify and forward relaying with adaptive modulation," in *Proc. 2009 IEEE PIMRC Spring*.

[11] S. Zhang, S. C. Liew, and P. P. Lam, "Hot topic: physical-layer network coding," in *Proc. 2006 ACM MobiCom*, pp. 358–365.

[12] T. Koike-Akino, P. Popovski, and V. Tarokh, "Optimized constellations for two-way wireless relaying with physical network coding," *IEEE J. Sel. Areas Commun.*, vol. 27, no. 5, pp. 773–787, 2009.

[13] H. J. Yang, Y. Choi, and J. Chun, "Modified high-order PAMs for binary coded physical-layer network coding," *IEEE Commun. Lett.*, vol. 14, no. 8, pp. 689–691, 2010.

[14] M. Noori and M. Ardakani, "On symbol mapping for binary physical layer network coding with PSK modulation," *IEEE Trans. Wireless Commun.*, vol. 11, no. 1, pp. 21–26, Jan. 2012.

[15] P. Larsson, N. Johansson, and K.-E. Sunell, "Coded bi-directional relaying," *2005 ADHOC*.

[16] X. Zhang, A. Ghrayeb, and M. Hasna, "On relay assignment in network coded cooperative systems," *IEEE Trans. Wireless Commun.*, vol. 10, no. 3, pp. 868–876, Mar. 2011.

[17] S. Nguyen, A. Ghrayeb, G. Al-Habian, and M. Hasna, "Mitigating error propagation in two-way relay channels with network coding," *IEEE Trans. Wireless Commun.*, vol. 9, no. 11, pp. 3380–3390, Nov. 2010.

[18] X. Zeng, A. Ghrayeb, and M. Hasna, "Joint optimal threshold-based relaying and ML detection in network-coded two-way relay channels," *IEEE Trans. Commun.*, vol. 60, no. 9, pp. 2657–2667, Sept. 2012.

[19] Y. Li, R. H. Y. Louie, and B. Vucetic, "Relay selection with network coding in two-way relay channels," *IEEE Trans. Veh. Technol.*, vol. 59, no. 9, pp. 4489–4499, Nov. 2010.

[20] S. Tang, H. Yomo, T. Ueda, R. Miura, and S. Obana, "Full rate network coding via nesting modulation constellations," *EURASIP J. WCN,* 2011.

[21] J. M. Park, S.-L. Kim, and J. Choi, "Hierarchically modulated network coding for asymmetric two-way relay systems," *IEEE Trans. Veh. Technol.*, vol. 59, June 2010.

[22] T. Wang, A. Cano, G. B. Giannakis, and F. Ramos, "Multi-tier cooperative broadcasting with hierarchical modulations," *IEEE Trans. Wireless Commun.*, vol. 6, pp. 3047–3057, Aug. 2007.

[23] M. Chang and S. Lee, "Performance analysis of cooperative communication system with hierarchical modulation over Rayleigh fading channel," *IEEE Trans. Wireless Commun.*, vol. 8, no. 6, pp. 2848–2852, Jun. 2009.

[24] C. Hausl and J. Hagenauer, "Relaying communication with hierarchical modulation," *IEEE Commun. Lett.*, vol. 11, pp. 64–66, Jan. 2007.

[25] Z. Yi and I.-M. Kim, "An opportunistic-based protocol for bidirectional cooperative networks," *IEEE Trans. Wireless Commun.*, vol. 8, no. 9, pp. 4836–4847, Sep. 2009.

[26] M. Ju and I.-M. Kim, "Joint relay selection and opportunistic source selection in bidirectional cooperative diversity networks," *IEEE Trans. Veh. Technol.*, vol. 59, no. 6, pp. 2885–2897, Jul. 2010.

[27] T. Wang, A. Cano, G. B. Giannakis, and J. N. Laneman, "High-performance cooperative demodulation with decode-and-forward relays," *IEEE Trans. Commun.*, vol. 55, no. 7, pp. 1427–1438, July 2007.

[28] P. K. Vitthaladevuni and M.-S. Alouini, "A recursive algorithm for the exact BER computation of generalized hierarchical QAM constellations," *IEEE Trans. Inf. Theory*, vol. 49, no. 1, pp. 297–307, Jan. 2003.

[29] K. Tourki, H.-C. Yang, and M.-S. Alouini, "Accurate outage analysis of incremental decode-and-forward opportunistic relaying," *IEEE Trans. Wireless Commun.*, vol. 8, no. 9, pp. 4836–4847, Sep. 2009.

Xuehua Zhang received her M.A.Sc degree in electrical engineering from the Concordia University, Montreal, QC, Canada in 2010. She is currently working toward the Ph.D. degree in electrical engineering at Concordia University. Her current research interests include wireless communications, cooperative communications and network coding.

Ali Ghrayeb (S'97-M'00-SM'06) received the Ph.D. degree in electrical engineering from the University of Arizona, Tucson, USA in 2000. He is currently a Professor with the Department of Electrical and Computer Engineering, Texas A&M University at Qatar (on leave from Concordia University, Montreal, Canada.)

He is a co-recipient of the IEEE Globecom 2010 Best Paper Award. He is the coauthor of the book Coding for MIMO Communication Systems (Wiley, 2008). His research interests include wireless and mobile communications, error correcting coding, MIMO systems, wireless cooperative networks, and cognitive radio systems.

Dr. Ghrayeb has instructed/co-instructed technical tutorials at several major IEEE conferences. He served as the TPC co-chair of the Communications Theory Symposium of IEEE Globecom 2011. He is serving as the TPC co-chair of the 2016 IEEE WCNC conference. He serves as an Editor of the IEEE TRANSACTIONS ON WIRELESS COMMUNICATIONS, and the IEEE TRANSACTIONS ON COMMUNICATIONS. He served as an Associate Editor of IEEE TRANSACTIONS ON SIGNAL PROCESSING, IEEE TRANSACTIONS ON VEHICULAR TECHNOLOGY, the *Elsevier Physical Communications*, and the *Wiley Wireless Communications and Mobile Computing Journal.*

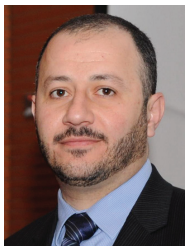

Mazen O. Hasna (S'94-M'03-SM'08) received the bachelor degree from Qatar University, Doha, Qatar in 1994, the master's degree from the University of Southern California (USC), Los Angeles in 1998, and the Ph.D. degree from the University of Minnesota, Twin Cities in 2003, all in electrical engineering.

In 2003, Dr. Hasna joined the electrical engineering department at Qatar University as an assistant professor. Currently, he serves as the Dean of Engineering at Qatar University.

Dr. Hasna's research interests span the general area of digital communication theory and its application to performance evaluation of wireless communication systems over fading channels. Current specific research interests include cooperative communications, ad hoc networks, cognitive radio, and network coding.